A Three-Dimensional Spatial Fading Correlation Model for Uniform Rectangular Arrays

S. K. Yong, *Student Member, IEEE,* and J. S. Thompson, *Member, IEEE*

***Abstract*—In this letter, a closed-form expression for the spatial fading correlation function of a uniform rectangular array (URA) in a three-dimensional (3-D) multipath channel is derived. The fading correlation function is expressed in terms of both the azimuth and elevation angle of arrival as well as the antenna spacing and geometry of the URA. Verification is achieved by means of computer simulation where the theoretical and simulation results are shown to be in good agreement. Our results demonstrate that azimuth spread (AS) is the primary determinant of the antenna correlation and the impact of the elevation spread is mainly noticeable at low AS values. The results obtained in this letter are vital for capacity analysis in multiple-input multiple-output systems, as well as for sensitivity analysis of the antenna array under study.**

***Index Terms*—Azimuth spread, elevation spread, radio propagation, spatial fading correlation, uniform rectangular arrays (URA).**

I. Introduction

ANTENNA arrays (AAs) are one of the most promising candidates for capacity and signal quality enhancement in wireless communications systems. Since the functionality of the AA is mainly based on the exploitation of the spatial properties of the multipath channel, it is imperative to gain a good understanding of the influence of angular parameters on the performance of AAs. In general, the angular domain comprises both the azimuth-of-arrival (AOA) and elevation-of-arrival (EOA). One investigation that incorporates a three-dimensional (3-D) approach has been reported in [1], where the author assumed that AOA is uniformly distributed over $[0, 2\pi]$, while the EOA is nonuniformly distributed around the horizontal plane. The spatial correlation (SC) is expressed in terms of an integral of a Bessel function of first kind of zero order. However, no closed-form expression is given in [1] to relate different parameters associated with AOA, EOA, and the geometry of the AA so that the SC can be easily evaluated. Such a closed-form expression is needed to simplify the analyses of the impact of these parameters on the system performance. Recent results in [2], [3] demonstrate that it is not always true to assume isotropic scattering, particularly in dense urban areas with street dominated environments where the *canyon effect* is significant. Moreover, in AA terminal receivers, the beamforming algorithm itself will determine the effective angle spread that is being observed.

Manuscript received June 30, 2003; revised August 22, 2003. This work was supported by Virtual Centre of Excellence in Mobile and Personal Communications (Mobile VCE).

The authors are with the Institute for Digital Communications, University of Edinburgh, Edinburgh EH9 3JL, U.K. (e-mail: ysk@ieee.org).

Digital Object Identifier 10.1109/LAWP.2003.819666

Prior works such as [4] and [5] expressed the SC functions for the case of uniform linear arrays and uniform circular arrays under uniform and Laplacian AOA probability density functions (pdfs). While the results in these works are important for diversity studies, they are limited to the azimuth plane only. Here, we consider the impact of both the AOA and the EOA on the SC for uniform rectangular arrays (URA). Our analysis is important as the performance of the handset AAs is also dependent on the effect of EOA since the handset could be randomly oriented [6]. Furthermore, recent measurement results have also demonstrated the significance of the EOA where [2] reported that about 65% of the energy was incident with elevation larger than 10° with respect to azimuth plane. Interestingly, [3] reported an average elevation spread (ES) of 9° for several environments ranging from indoor to outdoor. The major applications of our work are twofold. First, for capacity analysis in multiple-input multiple-output (MIMO) systems as the developed SC function can be applied to determine the correlation matrix at both the base station (BS) and mobile station (MS) [7]. Second, to study the sensitivity of the AA under various channel conditions as demonstrated in [8]. These applications further emphasize the importance of our work. This letter is organized as follows: Section II describes the directional channel model and the steering vector (SV) of the URA; Section III derives the closed-form expression for the spatial fading correlation function in terms of AOA, EOA, antenna spacing, and antenna geometry; Section IV presents some analytical and simulation results to highlight the impact of both the AOA and EOA on the SC. Finally, in Section V, some concluding remarks are drawn.

II. Directional Channel Model

In this letter, the performance analysis is done by using a frequency nonselective directional Rayleigh fading channel model. The channel impulse response, $\boldsymbol{h}(t)$ can be expressed as

$$\boldsymbol{h}(t) = \sum_{l=1}^{L} \alpha_l(t) \cdot \boldsymbol{a}(\varphi_l, \theta_l) \tag{1}$$

where L is the total number of multipath components (MPCs), $\alpha_l(t)$ is the complex amplitude of the l^{th} MPC, $\boldsymbol{a}(\varphi_l, \theta_l)$ is the SV of the URA, where the scalars $0 \leq \varphi_l < 2\pi$ and $0 \leq \theta_l < \pi$ are the azimuth and elevation angles of the l^{th} MPC defined with respect to the positive x- and z-axis, respectively, as illustrated in Fig. 1. For a size $N \times P$ URA located in the x-y plane with

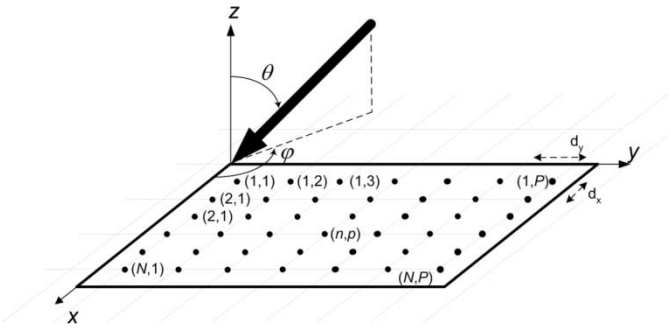

Fig. 1. Plane wave propagation where the incoming signal paths are at a discrete MAOA, AS, MEOA, and ES.

the phase reference at the origin, the SV for the azimuth, φ and elevation, θ is given by

$$\begin{aligned}\boldsymbol{a}(\varphi,\theta) &= \mathrm{vec}(\boldsymbol{a}_N(\mu)\boldsymbol{a}_P^T(\upsilon)) \\ &= \Big[1,\, e^{j\upsilon},\ldots,e^{j(P-1)\upsilon},e^{j\mu},e^{j(\mu+\upsilon)},\ldots, \\ &\quad e^{j[\mu+(P-1)\upsilon]},\ldots,e^{j(N-1)\mu},\ldots,e^{j[(N-1)\mu+(P-1)\upsilon]}\Big]^T\end{aligned} \tag{2}$$

where $\mu = 2\pi d_x \cos\varphi \sin\theta/\lambda$, $\upsilon = 2\pi d_y \sin\varphi\sin\theta/\lambda$, $\boldsymbol{a}_N(\mu) = \left[1, e^{j\mu},\ldots,e^{j(N-1)\mu}\right]^T$, and $\boldsymbol{a}_P(\upsilon) = \left[1, e^{j\upsilon},\ldots,e^{j(P-1)\upsilon}\right]^T$. The notation $[\cdot]^T$ denotes the transpose and λ is the wavelength. The scalars d_x and d_y are the spacings between the array elements parallel to the x- and y-axis, respectively. The operator $\mathrm{vec}(\cdot)$ maps the $N \times P$ matrix to an $NP\times 1$ vector by stacking the columns of the matrix. The index n and p refer to the antenna element located at n^{th} row and p^{th} column of the URA, denoted as (n,p).

III. Spatial Fading Correlation

The spatial fading correlation between antennas at positions (n,p) and (m,q) is defined as

$$\begin{aligned}\rho_{[(n,p),(m,q)]} &= E\left[a_{np}(\varphi,\theta)a_{mq}^*(\varphi,\theta)\right] \\ &= \int_\varphi\int_\theta a_{np}(\varphi,\theta)a_{mq}^*(\varphi,\theta)p(\varphi,\theta)\sin(\theta)d\theta d\varphi\end{aligned} \tag{3}$$

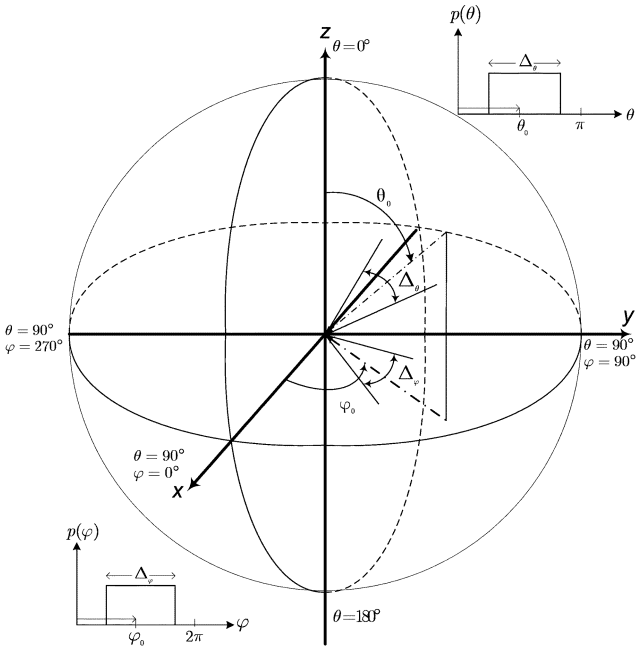

Fig. 2. Illustration of the MAOA, AS, MEOA, and ES used throughout the analysis.

where $E[\cdot]$ denotes expectation, the superscript * denotes the complex conjugate and $a_{np}(\varphi,\theta)$ is the (n,p) entry of $\boldsymbol{a}(\varphi,\theta)$. The scalar $p(\varphi,\theta)$ is the joint pdf of the angles of arrival of the MPC. Assuming that the AOA and EOA are independent of each other, the function $p(\varphi,\theta)$ can be decomposed to $p(\varphi)p(\theta)$. We concentrate our analysis on uniform AOA and EOA distributions since [9] shows that the key parameter to the system performance is the spread of the MPC and not the type of pdf under investigation. As shown in the Appendix , the real and imaginary part of the $\rho_{[(n,p),(m,q)]}$ can be expressed as (4) and (5), respectively, shown at the bottom of the page, where Δ_θ, Δ_φ, θ_{o} and φ_{o} are the ES, azimuth spread (AS), mean elevation-of-arrival (MEOA), and mean azimuth-of-arrival (MAOA), respectively. The scalars $\alpha = \varphi_0 + \gamma$ and Z are defined in the Appendix . Throughout our analysis, the AS and ES are defined as the maximum deviation of the angle spread from the MAOA and MEOA, respectively, as depicted in Fig. 2. Using

$$\begin{aligned}&\mathrm{Re}\left\{\rho_{[(n,p),(m,q)]}\right\} = \\ &\frac{-1}{\mathrm{sinc}(\Delta_\theta)\sin(\theta_0)}\left\{\sum_{k=0}^{\infty}\sum_{l=0}^{k}\frac{(-1)^{2k+1+l}Z^{2k}}{2^{4k}(k!)^2}\binom{2k+1}{l}\mathrm{sinc}\left[(2k+1-2l)\Delta_\theta\right]\sin\left[(2k+1-2l)\theta_0\right]\right. \\ &\left.+2\sum_{k=1}^{\infty}\sum_{l=0}^{\infty}\sum_{p=0}^{k+l}\frac{(-1)^{k+2l+1+p}}{l!\Gamma(2k+l+1)}\left(\frac{Z^{2(k+l)}}{2^{4(k+l)}}\right)\mathrm{sinc}(2k\Delta_\varphi)\cos(2k\alpha)\mathrm{sinc}[[2(k+l-p)+1]\Delta_\theta]\sin\left[[2(k+l-p)+1]\theta_0\right]\binom{2(k+l)+1}{p}\right\}\end{aligned} \tag{4}$$

$$\begin{aligned}&\mathrm{Im}\left\{\rho_{[(n,p),(m,q)]}\right\} = \\ &\frac{2}{\mathrm{sinc}(\Delta_\theta)\sin(\theta_0)}\sum_{k=0}^{\infty}\sum_{l=0}^{\infty}\sum_{p=0}^{k+l}\frac{(-1)^l}{l!\Gamma(2k+l+2)}\times\left(\frac{Z}{2}\right)^{2(k+l)+1}\mathrm{sinc}\left[(2k+1)\Delta_\varphi\right]\sin\left[(2k+1)\alpha\right] \\ &\times\left\{\frac{1}{2^{2(k+l+1)}}\binom{2(k+l+1)}{l+k+1}+\frac{(-1)^{k+l+1+p}}{2^{2(k+l)+1}}\binom{2(k+l+1)}{p}\mathrm{sinc}\left[2(k+l+1-p)\Delta_\theta\right]\cos\left[2(k+l+1-p)\theta_0\right]\right\}\end{aligned} \tag{5}$$

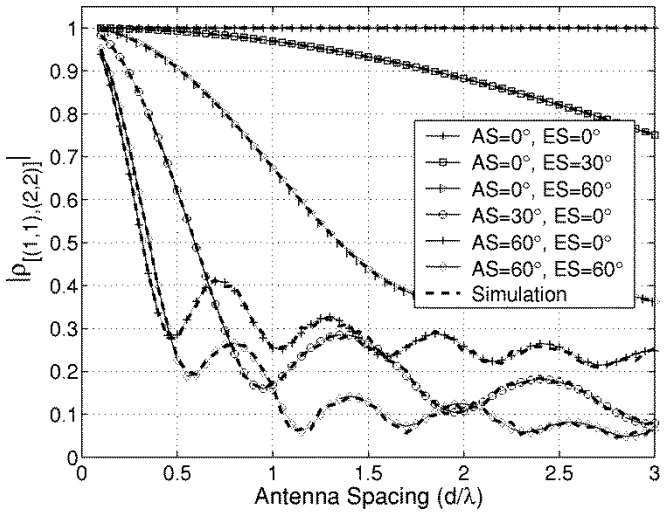

Fig. 3. SC at various AS and ES values with 90° MEOA and MAOA.

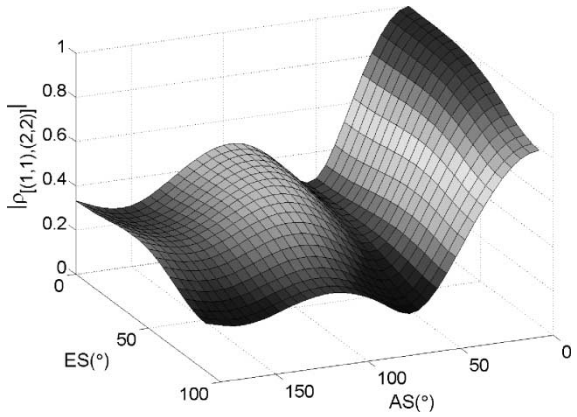

Fig. 4. SC as a function of both AS and ES at 90° MAOA and MEOA with 0.5λ spacing.

the definition in [4], the AOAs of the MPCs are uniformly distributed over the range of angles $[\varphi_0 - \Delta_\varphi, \varphi_0 + \Delta_\varphi]$. Similarly, the EOAs of the MPCs are also uniformly distributed over $[\theta_0 - \Delta_\theta, \theta_0 + \Delta_\theta]$. Note that the developed SC function is computationally efficient: summation over 50 terms for k and l is sufficient to achieve accuracy up to six decimal places when comparing (4) and (5) with numerical integration of (8) and (9), respectively.

IV. Analytical Results

In this section, some analytical results are presented and compared with simulation results. For all cases, simulation has been performed over 3 000 000 channel realizations to calculate the correlation values and these results validate the derived expression. Furthermore, the impact of both the AOA and the EOA is compared to identify the importance of these two parameters to the system performance. Fig. 3 shows the SC, $|\rho_{[(n,p),(m,q)]}|$ between antennas (1,1) and (2,2) as a function of antenna spacing with $d = d_x = d_y$ for different AS and ES values, at 90° MAOA and MEOA. It can be observed that as the AS and ES increase, the SC decreases. For the same increment in both AS and ES, the SC reduces more rapidly in the case of the AS. This suggests that the impact of AS on the SC is more significant than that of ES. To account for the joint contribution of both parameters on SC, we present theoretical results for the SC at 0.5λ spacing, 90° MAOA and MEOA with varying AS and ES values as illustrated in Fig. 4. It can be noted that the rate at which the SC drops with respect to the ES is somewhat less than the AS case.

V. Conclusion

In this letter, a closed-form expression for the spatial fading correlation function in terms of MAOA, AS, MEOA, ES, antenna spacing, and geometry of the URA is derived. The theoretical results are verified by means of computer simulation, where both results show excellent agreement. The developed SC is useful for capacity analysis in MIMO systems as it can used to determine the covariance matrix at both the BS and MS. Furthermore, the closed-form SC can also be used to study the array sensitivity under various channel conditions. While our results demonstrate that AS is the primary determinant of the SC, the SC is reduced somewhat as the ES increases, an effect that will impact the performance most dramatically when AS is small. Therefore, we emphasize that for an accurate system performance analysis, both AOA and EOA must be taken into consideration.

Appendix

From (3), the SC between the antenna elements (n, p) and (m, q) of the URA can be expressed as shown in (6) at the bottom of the page, where $C = 1/4\Delta_\varphi \sin(\theta_0)\sin(\Delta_\theta)$ $Z_x = 2\pi d_x(n-m)/\lambda$ and $Z_y = 2\pi d_y(p-q)/\lambda$. Let $Z = \sqrt{Z_x^2 + Z_y^2}$ and $\gamma = \tan^{-1}(Z_x/Z_y)$, then (6) can be rewritten as (7), shown at the top of the next page, where $\psi = \varphi + \gamma$. By making use of the well-known series [1], the real part and imaginary part of $\rho_{[(n,p),(m,q)]}$ can be further expressed as (8) and (9), shown at the top of the next page.

$$\begin{aligned}\rho_{[(n,p),(m,q)]} &= \int_\varphi \int_\theta a_{np}(\varphi,\theta) a^*_{mq}(\varphi,\theta) p(\varphi,\theta)\sin(\theta) d\theta d\varphi \\ &= C \int_{\varphi_0-\Delta\varphi}^{\varphi_0+\Delta\varphi} \int_{\theta_0-\Delta_\theta}^{\theta_0+\Delta_\theta} \left\{ e^{j2\pi/\lambda[(p-q)d_y \sin\varphi \sin\theta]} e^{j2\pi/\lambda[(n-m)d_x \cos\varphi \sin\theta]} \sin(\theta) \right\} d\theta d\varphi \\ &= C \int_{\varphi_0-\Delta\varphi}^{\varphi_0+\Delta\varphi} \int_{\theta_0-\Delta_\theta}^{\theta_0+\Delta_\theta} \left\{ e^{jZ_y \sin\theta \sin\varphi} e^{jZ_x \sin\theta \cos\varphi} \sin(\theta) \right\} d\theta d\varphi \end{aligned} \quad (6)$$

$$\begin{aligned}\rho_{[(n,p),(m,q)]} &= C\int_{\varphi_0-\Delta\varphi}^{\varphi_0+\Delta\varphi}\int_{\theta_0-\Delta_\theta}^{\theta_0+\Delta_\theta} e^{jZ\sin\theta\sin(\gamma+\varphi)}\sin(\theta)d\theta d\varphi \\ &= C\int_{\varphi_0+\gamma-\Delta\varphi}^{\varphi_0+\gamma+\Delta\varphi}\int_{\theta_0-\Delta_\theta}^{\theta_0+\Delta_\theta} e^{jZ\sin\theta\sin(\psi)}\sin(\theta)d\theta d\varphi \\ &= C\int_{\varphi_0+\gamma-\Delta\varphi}^{\varphi_0+\gamma+\Delta\varphi}\int_{\theta_0-\Delta_\theta}^{\theta_0+\Delta_\theta} \{\cos[Z\sin\theta\cos\psi]+j\sin[Z\sin\theta\sin(\psi)]\}\sin(\theta)d\theta d\psi \end{aligned} \tag{7}$$

$$\mathrm{Re}\left\{\rho_{[(n,p),(m,q)]}\right\} = C\int_{\varphi_0+\gamma-\Delta\varphi}^{\varphi_0+\gamma+\Delta\varphi}\int_{\theta_0-\Delta_\theta}^{\theta_0+\Delta_\theta}\left\{J_0(Z\sin\theta)+2\sum_{k=1}^{\infty}J_{2k}(Z\sin\theta)\cos(2k\psi)\sin(\theta)d\theta d\psi\right\} \tag{8}$$

$$\mathrm{Im}\left\{\rho_{[(n,p),(m,q)]}\right\} = C\int_{\varphi_0+\gamma-\Delta\varphi}^{\varphi_0+\gamma+\Delta\varphi}\int_{\theta_0-\Delta_\theta}^{\theta_0+\Delta_\theta} 2\sum_{k=1}^{\infty}J_{2k+1}(Z\sin\theta)\sin[(2k+1)\psi)]\sin(\theta)d\theta d\psi. \tag{9}$$

In order to evaluate these double integrals we first substitute for the Bessel functions in (8) and (9), using the following infinite series [10]

$$J_0(Z) = \sum_{k=0}^{\infty}(-1)^k\frac{Z^{2k}}{2^{2k}(k!)^2} \tag{10}$$

$$J_v(Z) = \left(\frac{Z}{2}\right)^v\sum_{k=0}^{\infty}\frac{(-1)^k}{(k!)\Gamma(v+k+1)}\left(\frac{Z}{2}\right)^{2k} \tag{11}$$

where $\Gamma(\cdot)$ is a gamma function. These series converge rapidly for small values of Z. The use of these series should be satisfactory when considering antenna spacings of practical interest, i.e., up to several carrier wavelengths. Second, we use the following indefinite integrals for power of trigonometric functions in (12) and (13) [10] to obtain the closed-form expressions of (4) and (5)

$$\int\sin^{2n}x dx = \frac{1}{2^{2n}}\binom{2n}{n}x + \frac{(-1)^n}{2^{2n-1}} \times\sum_{k=0}^{n-1}(-1)^k\binom{2n}{k}\frac{\sin(2n-2k)x}{2n-2k} \tag{12}$$

$$\int\sin^{2n+1}x dx = \frac{1}{2^{2n}}(-1)^{n+1}\sum_{k=0}^{n}(-1)^k \times\binom{2n+1}{k}\frac{\cos(2n+1-2k)x}{2n+1-2k}. \tag{13}$$

REFERENCES

[1] T. Aulin, "A modified model for the fading signal at the mobile radio channel," *IEEE Trans. Veh. Technol.*, vol. 28, pp. 182–202, Aug. 1979.

[2] A. Kuchar, J. P. Rossi, and E. Bonek, "Directional macro-cell channel characterization from urban measurements," *IEEE Trans. Antennas Propagat.*, vol. 48, pp. 137–146, Feb. 2000.

[3] K. Kalliola, K. Sulonen, H. Laitinen, O. Kivekas, J. Krogerus, and P. Vainikainen, "Angular power distribution and mean effective gain of mobile antenna in different propagation environments," *IEEE Trans. Veh. Technol.*, vol. 51, pp. 823–838, Sept. 2002.

[4] J. Salz and J. H. Winters, "Effect of fading correlation on adaptive arrays in digital mobile radio," *IEEE Trans. Veh. Technol.*, vol. 43, pp. 1049–1057, Nov. 1994.

[5] J.-A. Tsai, R. B. Buehrer, and B. D. Woerner, "Spatial fading correlation function of circular antenna arrays with Laplacian distribution energy," *IEEE Commun. Lett.*, vol. 6, pp. 178–180, May 2002.

[6] P. C. F. Eggers, I. Z. Kovác, and K. Olesen, "Penetration effects on XPD with GSM 1800 handset antennas, relevant for BS polarization diversity for indoor coverage," *Proc. IEEE Vehicular Technology Conf.—Spring*, vol. 13, pp. 1959–1963, May 1998.

[7] J. P. Kermoal, L. Schumacher, K. I. Pedersen, P. E. Mogensen, and F. Federiksen, "A stochastic MIMO radio channel model with experiment validation," *IEEE J. Select. Areas Commun.*, vol. 20, pp. 1211–1226, Aug. 2002.

[8] S. K. Yong and J. S. Thompson, "The effect of various channel conditions on the performance of different antenna arrays architectures," in *Proc. IEEE Vehicular Technology Conf.—Fall 2003*, to be published.

[9] J. B. Andersen and K. I. Pedersen, "Angle-of-arrival statistics for low resolution antenna," *IEEE Trans. Antennas Propagat.*, vol. 50, pp. 391–395, Mar. 2002.

[10] I. S. Gradshteyn and I. M. Ryzhik, *Table of Integrals, Series and Products*, 5th ed. New York: Academic, 1994.